

## Fundamental absorption edges in heteroepitaxial YBiO<sub>3</sub> thin films

Marcus Jenderka, Steffen Richter, Michael Lorenz, and Marius Grundmann

Citation: *Journal of Applied Physics* **120**, 125702 (2016); doi: 10.1063/1.4962975

View online: <https://doi.org/10.1063/1.4962975>

View Table of Contents: <http://aip.scitation.org/toc/jap/120/12>

Published by the [American Institute of Physics](#)

---

### Articles you may be interested in

[Laser-induced fluorescence analysis of plasmas for epitaxial growth of YBiO<sub>3</sub> films with pulsed laser deposition](#)

*APL Materials* **4**, 126102 (2016); 10.1063/1.4971349

[Double-layer buffer template to grow commensurate epitaxial BaBiO<sub>3</sub> thin films](#)

*APL Materials* **4**, 126106 (2016); 10.1063/1.4972133

[Tuning the electronic properties at the surface of BaBiO<sub>3</sub> thin films](#)

*AIP Advances* **6**, 065310 (2016); 10.1063/1.4954037

[Temperature dependent self-compensation in Al- and Ga-doped Mg<sub>0.05</sub>Zn<sub>0.95</sub>O thin films grown by pulsed laser deposition](#)

*Journal of Applied Physics* **120**, 205703 (2016); 10.1063/1.4968544

[Charge transfer-induced magnetic exchange bias and electron localization in \(111\)- and \(001\)-oriented LaNiO<sub>3</sub>/LaMnO<sub>3</sub> superlattices](#)

*Applied Physics Letters* **110**, 102403 (2017); 10.1063/1.4978358

[Electronic excitations and structure of Li<sub>2</sub>IrO<sub>3</sub> thin films grown on ZrO<sub>2</sub>:Y \(001\) substrates](#)

*Journal of Applied Physics* **117**, 025304 (2015); 10.1063/1.4905790

---

**AIP** | Journal of  
Applied Physics

SPECIAL TOPICS



## Fundamental absorption edges in heteroepitaxial YBiO<sub>3</sub> thin films

Marcus Jenderka,<sup>a)</sup> Steffen Richter, Michael Lorenz, and Marius Grundmann<sup>b)</sup>

*Institut für Experimentelle Physik II, Universität Leipzig, Linnéstraße 5, D-04103 Leipzig, Germany*

(Received 6 June 2016; accepted 6 September 2016; published online 23 September 2016)

The dielectric function of heteroepitaxial YBiO<sub>3</sub> grown on *a*-Al<sub>2</sub>O<sub>3</sub> single crystals via pulsed laser deposition is determined in the spectral range from 0.03 eV to 4.5 eV by a simultaneous modeling of the spectroscopic ellipsometry and optical transmission data of YBiO<sub>3</sub> films of different thicknesses. The (111)-oriented YBiO<sub>3</sub> films are nominally unstrained and crystallize in a defective fluorite-type structure with a *Fm* $\bar{3}$ *m* space group. From the calculated absorption spectrum, a direct electronic bandgap energy of 3.6(1) eV and the signature of an indirect electronic transition around 0.5 eV are obtained. These values provide necessary experimental feedback to previous conflicting electronic band structure calculations predicting either a topologically trivial or a non-trivial insulating ground state in YBiO<sub>3</sub>. *Published by AIP Publishing.* [<http://dx.doi.org/10.1063/1.4962975>]

### I. INTRODUCTION

During the past ten years, heteroepitaxial YBiO<sub>3</sub> thin films were investigated mainly as a buffer layer for the epitaxial YBa<sub>2</sub>Cu<sub>3</sub>O<sub>7- $\delta$</sub>  high-*T<sub>c</sub>* superconductors.<sup>1-4</sup> Recently, the first-principles electronic band structure calculations proposed YBiO<sub>3</sub> as a novel oxide topological insulator.<sup>5</sup> Based on an assumed, undistorted perovskite structure with a space group *Pm* $\bar{3}$ *m* and a lattice constant *a* = 5.428 Å, a topologically insulating phase was predicted due to a band inversion between an *s*-like and a *j<sub>eff</sub>* = 1/2 band at the *R* point that is driven by the spin-orbit coupling of the Bi *6p* states. YBiO<sub>3</sub> then has a topological trivial indirect bandgap of  $\approx$ 0.18 eV and a non-trivial direct bandgap of 0.33 eV at the *R* point. The size of the direct bandgap and high bulk resistivity were expected to allow for a surface-dominated transport at room-temperature. However, a subsequent theoretical study showed that the assumed *Pm* $\bar{3}$ *m* crystal structure is unstable.<sup>6</sup> Instead, a distorted *Pnma* perovskite structure is predicted to be most stable, and YBiO<sub>3</sub> is predicted as a topologically trivial band insulator with larger direct and indirect electronic bandgaps.

Experimentally, solid solutions of Y<sub>*x*</sub>Bi<sub>1-*x*</sub>O<sub>1.5</sub> with 0.1 < *x* < 0.5 are stable at room-temperature and crystallize in a face-centered cubic, defective fluorite-type structure with a space group *Fm* $\bar{3}$ *m*.<sup>7-10</sup> However, there exist no band structure calculations for the *Fm* $\bar{3}$ *m* space group. At *x* = 0.5, Y<sub>*x*</sub>Bi<sub>1-*x*</sub>O<sub>1.5</sub> (YBiO<sub>3</sub>) has a cubic lattice constant *a* = 5.4188 Å,<sup>10</sup> and its pseudo-cubic primitive cell with *a*/√2 is closely matched to LaAlO<sub>3</sub>, SrTiO<sub>3</sub>, (LaAlO<sub>3</sub>)<sub>0.3</sub>(Sr<sub>2</sub>TaAlO<sub>6</sub>)<sub>0.7</sub> (LSAT), and YBa<sub>2</sub>Cu<sub>3</sub>O<sub>7- $\delta$</sub> . Heteroepitaxial YBiO<sub>3</sub>(100) thin films have hence been prepared as buffer layers on LaAlO<sub>3</sub>(001), SrTiO<sub>3</sub>(001), and LSAT(001) single-crystalline substrates by chemical solution<sup>1-3</sup> and pulsed laser deposition (PLD).<sup>4,11</sup> Their surface-morphology is characterized by crystalline grains of around 50 nm and root-mean-squared (RMS) surface roughnesses between 2.6 and 1.8 nm at a film thickness of

140 and 40 nm, respectively.<sup>2,3</sup> Furthermore, pelletized YBiO<sub>3</sub> powders showed a high 0.5 MΩm bulk resistivity at room-temperature and a paramagnetic behavior.<sup>2</sup>

In order to provide some necessary experimental feedback to the conflicting theoretical band structure calculations,<sup>5,6</sup> we report here an estimate of the direct electronic bandgap of two relaxed-textured YBiO<sub>3</sub>(111) films deposited using pulsed laser deposition with different thickness on *a*-Al<sub>2</sub>O<sub>3</sub> single crystals. Structural analyses confirm their crystallization in a defective fluorite-type structure with a *Fm* $\bar{3}$ *m* space group. The dielectric function between 0.03 eV and 4.5 eV is determined by simultaneous modeling of the spectroscopic ellipsometry and optical transmission data. Contrary to the theoretical band structure calculations, we find evidence for a direct electronic bandgap of 3.6(1) eV and a possible signature of an indirect electronic transition around 0.5 eV in YBiO<sub>3</sub>.

### II. EXPERIMENTAL DETAILS

The YBiO<sub>3</sub> thin films were grown by pulsed laser deposition (PLD) on 10 × 10 mm<sup>2</sup> *a*-plane Al<sub>2</sub>O<sub>3</sub>(11-20) single crystals. PLD was performed with a 248 nm KrF excimer laser at a laser fluence of 2 Jcm<sup>-2</sup>. The polycrystalline source target was prepared by conventional solid-state synthesis of Bi<sub>2</sub>O<sub>3</sub> and Y<sub>2</sub>O<sub>3</sub> powders in a 1:1 molar ratio. The starting materials were homogenized, pressed, and sintered in air for 24 h at 880 °C. After an intermediate regrinding, the second and third sinter steps were performed for 12 h in an oxygen atmosphere at 800 °C and 1000 °C, respectively.

The deposition process involved a 300 laser pulses nucleation layer grown at a 1 Hz pulse frequency, followed by the deposition of 60 000 and 2000 pulses at 5 Hz for the thick and thin films, respectively. The films were grown at a growth temperature of approximately 650 °C and an oxygen partial pressure of 0.05 mbar to obtain optimal Y:Bi stoichiometry and film crystallinity. After the deposition, the samples were annealed *in situ* at an oxygen partial pressure of 800 mbar. The film thicknesses were determined as 1660 nm and 57 nm from an optical modeling (see text below). Note that reliable resistivity data were not obtained due to a very

<sup>a)</sup> Author to whom correspondence should be addressed. Electronic mail: [marcus.jenderka@physik.uni-leipzig.de](mailto:marcus.jenderka@physik.uni-leipzig.de)

<sup>b)</sup> URL: <http://research.uni-leipzig.de/hlp/>

large bulk resistance of the 1660 nm film of around 700 M $\Omega$  at room-temperature, which exceeds our instrument's measuring range.

The X-ray diffraction (XRD) structural analyses were performed with a Panalytical X'Pert PRO Materials Research Diffractometer with a parabolic mirror and a PIXcel<sup>3D</sup> detector and Cu K $\alpha$  radiation. The surface morphology was investigated with a Park Systems XE-150 atomic force microscope (AFM) in a dynamic non-contact mode. Topographic images were post-processed with the Gwyddion software.<sup>12</sup> The chemical composition was measured by energy-dispersive X-ray spectroscopy (EDX) using an FEI Novalab 200 scanning electron microscope (SEM) equipped with an Ametek EDAX detector. The thin film dielectric function and layer thickness were determined via standard variable angle spectroscopic ellipsometry (VASE, IR-VASE by J.A. Woolam, Inc.) in the spectral range from 0.03 eV to 4.50 eV and a UV/VIS transmission spectrometer (Perkin Elmer Lambda 19) between 0.62 eV and 6.20 eV.

### III. RESULTS AND DISCUSSION

#### A. Structural properties

Figure 1 shows an XRD  $2\theta$ - $\omega$ -scan of the polycrystalline YBiO<sub>3</sub> source target. The pattern is fit successfully by the Rietveld method<sup>13</sup> using the defective fluorite-type  $Fm\bar{3}m$  structural model by Zhang *et al.*<sup>10</sup> and a cubic lattice constant  $a = 5.4279(4)$  Å. There exist minor additional peaks that very likely relate to the unreacted starting materials and possibly elemental Bi and Bi<sub>2</sub>O<sub>3-x</sub>.<sup>3</sup> We note that the assumed  $Pm\bar{3}m$  and  $Pnma$  models fail to match with all of the observed YBiO<sub>3</sub> reflexes, see [supplementary material](#). EDX yields a Y:Bi ratio of 0.98:1, which suggests that a good stoichiometric transfer is feasible in spite of the incomplete target phase purity.

Figure 2(a) shows the  $2\theta$ - $\omega$  patterns of two YBiO<sub>3</sub> films with a thickness  $d$  of 1660 nm (film A) and 57 nm (film B), respectively, deposited on  $\alpha$ -Al<sub>2</sub>O<sub>3</sub> single crystals. The patterns are indexed according to the experimental  $Fm\bar{3}m$  unit cell<sup>7-10</sup> and indicate very good (111) preferential out-of-plane orientation. For film A, the pattern shows additional minor peaks (<10 cps) related to other allowed YBiO<sub>3</sub> reflexes. By an extrapolation of the  $\theta$  values of the (111),

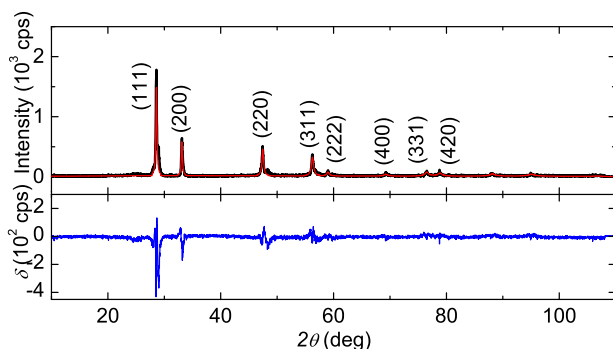


FIG. 1. Top: An XRD  $2\theta$ - $\omega$ -scan (black) of the polycrystalline YBiO<sub>3</sub> source target. The Rietveld method<sup>13</sup> is applied using the defective fluorite-type  $Fm\bar{3}m$  structural model<sup>10</sup> with  $a = 5.4279(4)$  Å. Bottom: difference  $\delta$  between the observed and calculated intensities.

(222) and, if possible, the (333) reflexes to  $\theta = 0^\circ$ ,<sup>14</sup> very similar out-of-plane lattice constants  $a_{\text{out}}$  of 5.3907(2) Å and 5.42(4) Å are determined for films A and B, respectively. These values deviate from the literature value of 5.4188 Å (Ref. 10) and from the Rietveld-refined value of the polycrystalline target by at most 0.5 and 0.7%, respectively.

For both films, the XRD  $\omega$ -scans (rocking scans) of the YBiO<sub>3</sub> (111) reflex (see Fig. 2(b)) exhibit identical half-widths of about 5° and, thus, suggest a comparable degree of crystallite mosaicity.

A possible in-plane epitaxial relationship with  $\alpha$ -Al<sub>2</sub>O<sub>3</sub> was investigated by  $\phi$ - $\chi$  pole figures around the asymmetric YBiO<sub>3</sub> (200) reflex (see Figs. 2(c) and 2(d)). For both films A (c) and B (d), a distinct circular intensity maximum is evidence for a random distribution of the in-plane crystallite orientation. The lack of a defined in-plane epitaxial relationship is explained by the large lattice mismatch between YBiO<sub>3</sub>(111) and  $\alpha$ -Al<sub>2</sub>O<sub>3</sub> of about  $\pm 40\%$ .<sup>15</sup>

The XRD data indicate relaxed, i.e., nominally unstrained, growth of YBiO<sub>3</sub>(111) on  $\alpha$ -Al<sub>2</sub>O<sub>3</sub>. Thus, the observed preferential out-of-plane orientation suggests that the YBiO<sub>3</sub> (111) surface has the lowest formation energy. Because EDX analyses on both films yield nearly ideal Y:Bi ratios of 1.02:1, the slight deviations of the out-of-plane lattice constant from the literature<sup>10</sup> and the polycrystalline target value are likely caused by internal strain due to, e.g., oxygen vacancies.

#### B. Optical properties

The spectra of the dielectric function were determined from ellipsometry and optical transmission data of the relaxed grown YBiO<sub>3</sub> films A and B. The anisotropic transfer matrix model consists of a semi-infinite substrate and layers for the YBiO<sub>3</sub> film and the surface roughness using a Bruggeman effective medium approximation mixing the dielectric functions of YBiO<sub>3</sub> and air in a 1:1 ratio.<sup>16</sup> Interference effects within the film are intrinsically accounted for by the transfer matrix approach. Interferences within the substrate, however, are not considered. The dielectric functions of the films are modeled using a Kramers-Kronig consistent numerical B-spline model.<sup>17</sup> We note that film A was deposited on a double-sided polished substrate to avoid diffusive scattering in the optical transmission spectroscopy. The substrate backside was subsequently roughened mechanically in order to minimize back surface reflections in ellipsometry. The substrate of film B was single-sided polished. Its wavelength-dependent scattering by the backside roughness in the transmission measurement is corrected for by a reference transmission measurement of a bare double-sided polished substrate with the same thickness. Finally, the absorption coefficient  $\alpha$  is calculated from the numerical B-spline dielectric function.

Figures 3(a)–3(c) show the results of the simultaneous modeling of the reflection ellipsometry ( $\Psi$ ,  $\Delta$ ) and optical transmission ( $T$ ) data of the YBiO<sub>3</sub> films A and B. The numerical B-spline model reproduces the experimental data in the entire measured spectral range (a,b). Around 200 meV, layer thickness oscillations of the thick substrate are present. These oscillations were not considered in the model, since at

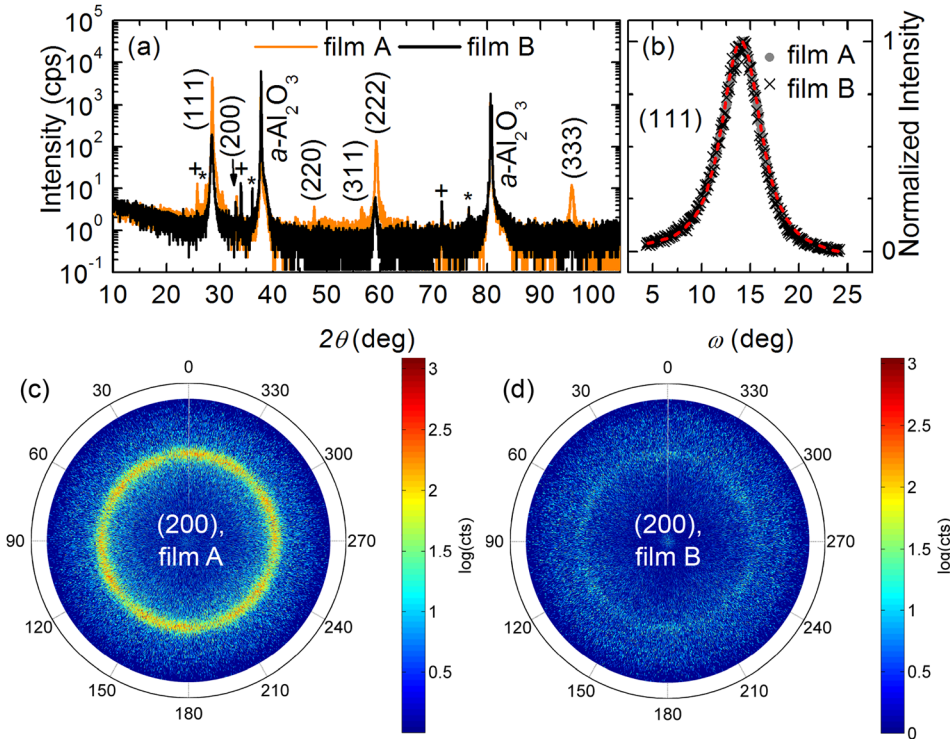


FIG. 2. XRD performed on the 1660 nm and 57 nm YBiO<sub>3</sub> films A and B deposited on *a*-Al<sub>2</sub>O<sub>3</sub>: (a) the  $2\theta$ - $\omega$  scans confirm an excellent (111) preferential out-of-plane orientation. Cu K $\beta$  and W lines are denoted by + and \*. (b) The normalized  $\omega$ -scans of the YBiO<sub>3</sub> (111) symmetric reflex with identical half-widths of 4.94(4) $^\circ$  obtained by a Gaussian fit (red dashed line). (c) and (d) The  $\phi$ - $\chi$  pole figures of the YBiO<sub>3</sub> (200) reflex indicate a nearly random distribution of the crystallite in-plane orientation in both films.

higher photon energies, they cannot be spectrally resolved, and at lower photon energies, the substrate is no longer transparent due to the Al<sub>2</sub>O<sub>3</sub> Reststrahlen band. The modeled  $T$  data of film B, Fig. 3(c), suffer from a large error as it was measured through a rough backside; in this case, the ellipsometry data are more reliable. The spectra of film A show obvious layer thickness oscillations of the YBiO<sub>3</sub> film. For films A and B, thicknesses of  $d = 1660(30)$  nm and  $d = 57(2)$  nm are obtained from the fits. The modeled effective surface roughnesses are approximately 25 nm and 3 nm, respectively. These values agree well with the surface roughness values obtained via the AFM (see [supplementary material](#)).

From the numerical model dielectric function, the absorption coefficient  $\alpha$  is calculated and plotted in Fig. 4 as  $\alpha(E)^2$  and  $\alpha(E)^{1/2}$ , respectively. Based on the present data, we can exclude the indirect and direct bandgaps at

$\approx 0.183$  eV and 0.33 eV, as predicted by the band structure calculations of Jin *et al.*<sup>5</sup> Instead, strong absorption is evident above 3 eV together with a continuous onset at about 0.5 eV. At about 0.05 eV, a phonon resonance is evident. The strong absorption peak is interpreted in analogy to Trimarchi *et al.*<sup>6</sup> as the allowed direct bandgap transition between the Bi 6*s* and 6*p* bands at the *R* point. For an estimate of the direct bandgap energy  $E_{\text{gd}}$ , a linear regression of the  $\alpha^2$  spectrum, Fig. 4(a), between 3.75 eV and 4.50 eV is performed.<sup>18</sup> The extrapolation of the straight line fit to 0 yields  $E_{\text{gd}} = 3.6(1)$  eV. Furthermore, we tentatively associate the slight absorption starting at around 0.5 eV, visible in Fig. 4(b), with the allowed indirect bandgap transition from the valence band maximum at the  $\Gamma$  point to the conduction band minimum at the *R* point.<sup>6</sup> To cross-check the reliability of our model, we have also modeled films A and B

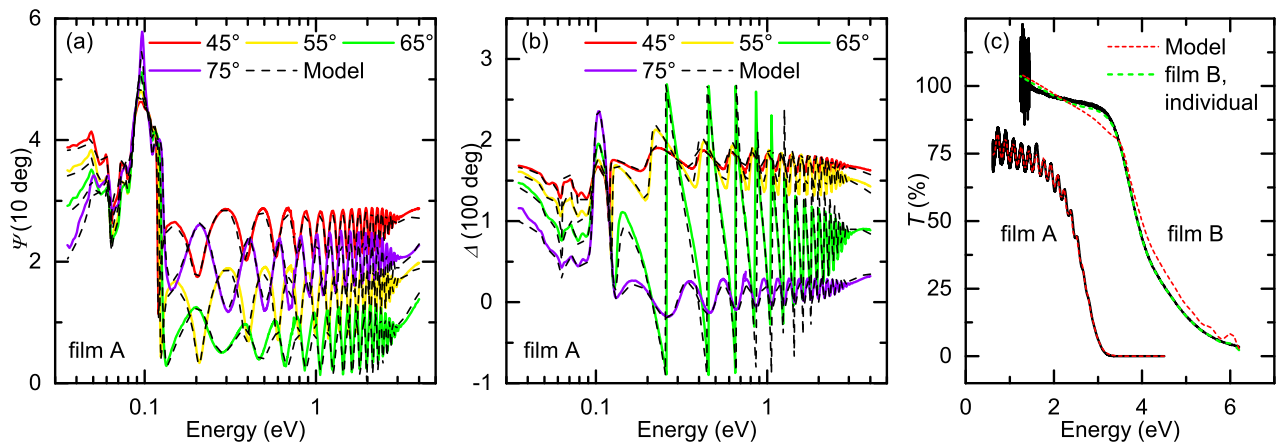


FIG. 3. The measured and model-calculated spectra of the ellipsometric parameters  $\Psi$  (a) and  $\Delta$  (b) of the 1660 nm thick YBiO<sub>3</sub> film A on *a*-Al<sub>2</sub>O<sub>3</sub> measured at angles of incidence as indicated. For  $\Psi$  and  $\Delta$  of the 57 nm film B, we refer to the supplementary material. (c) Optical transmission spectra  $T$  of films A and B (black) are shown together with the corresponding simultaneous model spectra (red). For comparison, the individual model spectrum of film B (green) is shown as well.

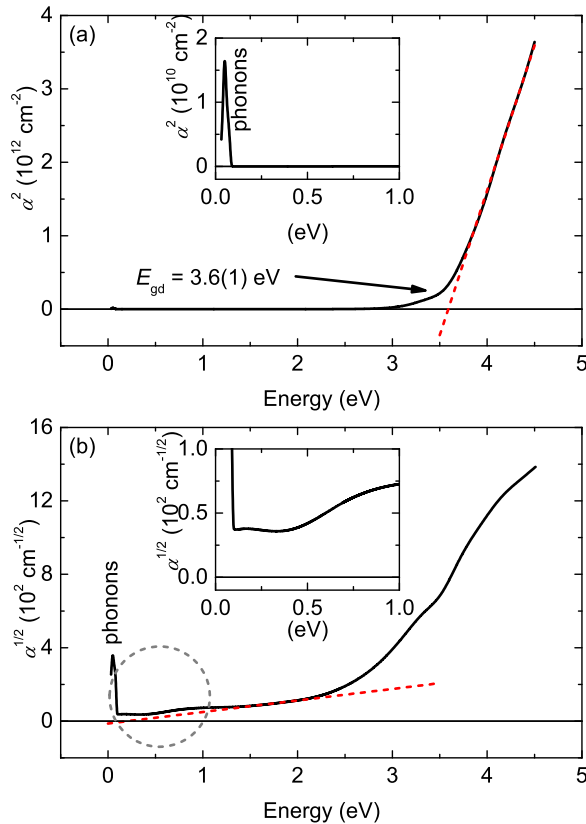


FIG. 4. The calculated absorption spectra plotted versus photon energy as  $\alpha^2$  (a) and  $\alpha^{1/2}$  (b). (a) A linear regression of  $\alpha^2$  between 3.75 eV and 4.50 eV and an extrapolation to  $\alpha^2=0$  yields an estimate of the direct bandgap of  $E_{gd}=3.6(1)$  eV. (b) The  $\alpha^{1/2}$  spectrum exhibits a phonon resonance at about 0.05 eV and a possible indirect bandgap absorption around 0.5 eV. The insets in (a) and (b) show a zoom-in of the 0 eV to 1 eV spectral range.

individually, as shown in the [supplementary material](#): While the model of the thin film B yields the same direct bandgap, cf. Fig. 3(c), but is insensitive to low-energy absorption, modeling of the thick film A is required to reveal a possible Urbach tail between 2.25 eV and 3.25 eV.

The obvious discrepancy between the predicted<sup>5,6</sup> and experimentally observed direct bandgap energy in YBiO<sub>3</sub> is not fully understood. Density functional theory models of a material's band structure typically underestimate the real bandgap by up to 40%.<sup>19</sup> However, the obtained bandgaps of the nominally unstrained YBiO<sub>3</sub> films seem reasonable as they linearly interpolate between the end members of the Y<sub>x</sub>Bi<sub>1-x</sub>O<sub>1.5</sub> solid solutions: While the as grown thin films of cubic  $\delta$ -Bi<sub>2</sub>O<sub>3</sub> have an indirect optical gap of 1.73 eV,<sup>20</sup> the pulsed laser-deposited cubic Y<sub>2</sub>O<sub>3</sub> thin films exhibit a direct bandgap of 5.6 eV.<sup>21</sup> In this light, the bowing effects in the band gap appear to be small.

#### IV. SUMMARY

In summary, we have prepared heteroepitaxial YBiO<sub>3</sub> films on *a*-Al<sub>2</sub>O<sub>3</sub> single crystals by pulsed laser deposition. A Rietveld refinement of the polycrystalline source target confirms that the defective fluorite-type structure with a space group  $Fm\bar{3}m$ <sup>7-10</sup> is the correct structural model for YBiO<sub>3</sub>. At film thicknesses of both 1660 nm and 57 nm, a

(111) preferential out-of-plane orientation is obtained. The X-ray diffraction analyses also confirm a relaxed and nominally unstrained film growth. In particular, there exists a random distribution of the in-plane crystallite orientation. The dielectric function is determined in the 0.03 eV–4.50 eV spectral range by simultaneous modeling of the spectroscopic ellipsometry and optical transmission data of both the film samples. From the calculated absorption coefficient, a direct electronic bandgap of 3.6(1) eV is obtained. We, furthermore, find a possible signature of another, indirect electronic transition around 0.5 eV. Together, these values provide necessary experimental feedback to electronic band structure calculations that have proposed either a topologically trivial<sup>6</sup> or a non-trivial<sup>5</sup> insulating ground state.

#### SUPPLEMENTARY MATERIAL

See [supplementary material](#) for further experimental details on Rietveld refinement, AFM and SEM images, and the simultaneous numerical B-spline model dielectric function.

#### ACKNOWLEDGMENTS

We thank the Deutsche Forschungsgemeinschaft (DFG) for financial support within the collaborative research project SFB 762 “Functionality of oxide interfaces.” S.R. is grateful to the Leipzig Graduate School of Natural Sciences BuildMoNa.

- <sup>1</sup>G. Li, M. Pu, X. Du, Y. Zhang, H. Zhou, and Y. Zhao, *Physica C* **452**, 43 (2007).
- <sup>2</sup>Y. Zhao, M. Pu, G. Li, X. Du, H. Zhou, Y. Zhang, X. Yang, Y. Wang, R. Sun, and C. Cheng, *Physica C* **463–465**, 574 (2007).
- <sup>3</sup>G. Pollefeyt, S. Rottiers, P. Vermeir, P. Lommens, R. Hühne, K. De Buysser, and I. Van Driessche, *J. Mater. Chem. A* **1**, 3613 (2013).
- <sup>4</sup>Y. Meiqiong, W. Xianhua, T. Yuancheng, and H. Junjun, *Chin. J. Vac. Sci. Technol.* **29**, 536–540 (2009).
- <sup>5</sup>H. Jin, S. H. Rhim, J. Im, and A. J. Freeman, *Sci. Rep.* **3**, 1651 (2013).
- <sup>6</sup>G. Trimarchi, X. Zhang, A. J. Freeman, and A. Zunger, *Phys. Rev. B* **90**, 161111 (2014).
- <sup>7</sup>P. D. Battle, C. R. A. Catlow, J. Drennan, and A. D. Murray, *J. Phys. C: Solid State Phys.* **16**, L561 (1983).
- <sup>8</sup>P. Battle, C. Catlow, J. Heap, and L. Moroney, *J. Solid State Chem.* **63**, 8 (1986).
- <sup>9</sup>K. V. Kale, K. M. Jadhav, and G. K. Bichile, *J. Mater. Sci. Lett.* **18**, 9 (1999).
- <sup>10</sup>X. J. Zhang, W. T. Jin, S. J. Hao, Y. Zhao, and H. Zhang, *J. Supercond. Novel Magn.* **23**, 1011 (2010).
- <sup>11</sup>R. de Putter, “Towards stoichiometric growth of YBiO<sub>3</sub> thin films using pulsed laser deposition: A plasma approach,” M.S. thesis, University of Twente, 2014.
- <sup>12</sup>D. Nečas and P. Klapetek, *Open Phys.* **10**, 181–188 (2012).
- <sup>13</sup>H. M. Rietveld, *J. Appl. Crystallogr.* **2**, 65 (1969).
- <sup>14</sup>J. B. Nelson and D. P. Riley, *Proc. Phys. Soc.* **57**, 160 (1945).
- <sup>15</sup>Assuming a cubic YBiO<sub>3</sub>(111) epilayer with  $a_{(111)} = \sqrt{2} \times 5.42 \text{ \AA}$ , the lattice mismatch with the  $13.00 \times 5.50 \text{ \AA}^2$  a-plane of Al<sub>2</sub>O<sub>3</sub> will be +42% and -40%, respectively.
- <sup>16</sup>D. A. G. Bruggeman, *Ann. Phys.* **416**, 636 (1935).
- <sup>17</sup>B. Johs and J. S. Hale, *Phys. Status Solidi A* **205**, 715 (2008).
- <sup>18</sup>H. Fujiwara, *Spectroscopic Ellipsometry: Principles and Applications* (John Wiley & Sons, Chichester, England; Hoboken, NJ, 2007).
- <sup>19</sup>J. P. Perdew, *Int. J. Quantum Chem.* **28**, 497 (2009).
- <sup>20</sup>H. T. Fan, S. S. Pan, X. M. Teng, C. Ye, and G. H. Li, *J. Phys. D: Appl. Phys.* **39**, 1939 (2006).
- <sup>21</sup>S. Zhang and R. Xiao, *J. Appl. Phys.* **83**, 3842 (1998).